Temperature-insensitive displacement sensor based on high-birefringence photonic crystal fiber loop mirror

Hao ZHANG[1*], Bo LIU[1], Zhi WANG[1], Jianhua LUO[2], Shuangxia WANG[2], Chenglai JIA[2], Xiurong MA[3]

[1]Key Laboratory of Opto-Electronic Information and Technology, Ministry of Education, Institute of Modern Optics, Nankai University, Tianjin 300071, P.R. China

[2]College of Information Technical Science, Nankai University, Tianjin 300071, P.R. China

[3]School of Electronics Information Engineering, Tianjin University of Technology 300191, P.R. China

*Corresponding author: haozhang@nankai.edu.cn; dr_haozhang@yahoo.com.cn

A temperature-insensitive displacement sensor based on high-birefringence photonic crystal fiber loop mirror (Hi-Bi PCFLM) is proposed. Through the measurement of transmission peak wavelength of the Hi-Bi PCFLM, this displacement sensor quantifies the free end displacement of a uniform-strength cantilever beam, on which part of Hi-Bi PCF is pasted. We have theoretically analyzed its operation principle, which is validated by our experimental results. This displacement sensor has the sensitivity of 0.28286 nm/mm and 0.27024 nm/mm over a range from –21 mm to 21 mm for two adjacent peak wavelengths, respectively. Experimental observation indicates that this sensor has good stability through a temperature range from 40 °C to 109.5 °C.

Keywords: fiber-optic sensor, displacement sensor, high-birefringence fiber loop mirror (Hi-Bi FLM), photonic crystal fiber (PCF), uniform-strength cantilever beam (UCB).

1. Introduction

Due to their simple structure, compact size, spectral flexibility and high sensitivity, high-birefringence fiber loop mirrors (Hi-Bi FLMs) have become a subject of extensive studies in the past several years. The comb-like spectrum of Hi-Bi FLMs results from the interference between the clockwise and counterclockwise beams propagating inside the fiber loop. They have found various applications in the field of optical communications as amplified spontaneous emission (ASE) rejecters in double--pass erbium-doped fiber amplifiers (EDFA) [1], gain flattening filters for EDFAs [2], and wavelength-selective components in multi-wavelength fiber lasers [3]. In the past decade, a lot of effort has been put on developing Hi-Bi-FLM-based sensors for the measurement of temperature [4], strain [5], liquid level [6], current [7], voltage [8], and multi-parameter sensing applications [9–12]. In particular, LIU *et al.*

investigated the reflection and transmission characteristics of the fiber loop mirrors based on conventional polarization maintaining fiber (PMF) and their applications in strain and temperature sensing [13]. In their paper, they designed a strain sensor based on the PMF-based FLM with part of the PMF pasted on a uniform-strength cantilever beam (UCB). With this sensor they could also establish the relationship between the free end displacement of the UCB and the transmission peak shift of the Hi-Bi fiber loop interferometer. However, a few papers report that the interference spectrum of Hi-Bi FLMs based on conventional PMF is sensitive to the environmental changes such as temperature, which will inevitably degrade the sensor performance [13–15]. Also, LIU *et al*., employed the PMF-based FLM as a temperature sensor and its temperature sensitivity reaches 0.9435 nm/°C. Since the PMF-based fiber loop interferometers have relatively large temperature sensitivity, it would be necessary to eliminate the temperature effect on its transmission spectrum for the measurement of strain or displacement in practical applications. And in this case, a temperature control system is indispensable to maintain a constant temperature environment for the Hi-Bi FLM sensor, which will considerably increase the system cost and technical complexity. The uprising of photonic crystal fibers (PCFs) provides a solution to the above issue. Unlike the conventional PMFs consisting of glasses with different thermal expansion coefficients, Hi-Bi PCFs are made of air-holes in only one type of glass, and therefore, the birefringence of PCF induced by geometrical asymmetry is highly insensitive to the environmental temperature changes. MICHIE *et al*. [16] reported the temperature independent modal birefringence of highly birefringent PCF. Moreover, ORTIGOSA-BLANCH *et al*. [17] investigated the dependence of dispersion and birefringence of a highly birefringent PCF, showing that PCFs exhibit no dependence of temperature owing to the single material nature of their structures. Due to its temperature independence characteristics, birefringent PCF was employed for the measurement of hydrostatic pressure and strain [18]. Furthermore, several studies have shown that the transmission characteristics of birefringent PCF-based fiber loop interferometers are temperature independent [19, 20] and the birefringent PCF-based FLMs have been extensively studied for the measurement of numerous parameters including strain [21–23], curvature [24], *etc*. As an extension of the sensing applications, the PCF-based FLM was also applied in the interrogation of fiber Bragg grating (FBG) sensors [25].

In this letter, a simple, low cost, and temperature-insensitive fiber-optic sensor for the measurement of displacement based on Hi-Bi PCFLM is proposed and experimentally demonstrated. A section of Hi-Bi PCF is pasted on a UCB. As the free end displacement of the UCB changes, the transmission spectrum of the Hi-Bi PCFLM will shift accordingly. Thereby, the relationship between the displacement and wavelength shift could be obtained. The operation principle of this displacement sensor is theoretically analyzed, and its stability has also been experimentally observed. Compared with Liu's work in reference [13], owing to the temperature insensitive nature of the Hi-Bi PCF, the proposed displacement sensor based on Hi-Bi PCFLM could be applied without the requirement of any additional temperature controlling

devices, which would economize the system cost to a large extend and improve the stability of the sensing system.

2. Experimental setup and operation principle

Figure 1 shows the schematic diagram of the Hi-Bi-PCFLM-based displacement sensing system with a photograph of the Hi-Bi PCF used in our experiment. A C-band erbium-doped broadband source is utilized as the light source. About 11.2 cm Hi-Bi PCF and a polarization controller are placed between two coupling arms of a 3-dB coupler to constitute the Hi-Bi PCFLM. The birefringence of PCF is introduced by its geometric asymmetry, as shown in the inset of Fig. 1. There are two large holes with
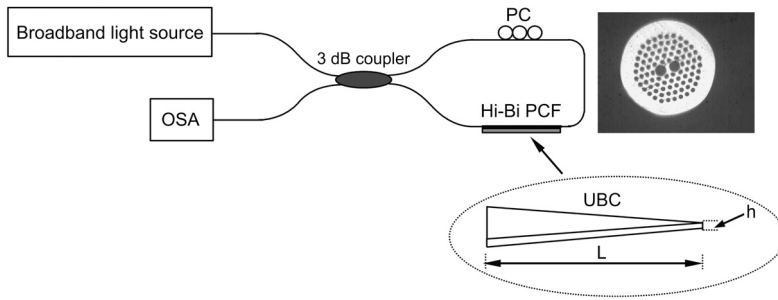

Fig. 1. Schematic diagram of the Hi-Bi-PCFLM-based sensing system with a photograph of the Hi-Bi PCF.

the diameter of 14.16 µm in the central area of the PCF and smaller air holes with the diameter of 5.64 µm periodically arranged in the cladding area. The spacing between the large air holes is 19.88 µm, and the pitch of the small air holes is 9.25 µm. The operation principle of the Hi-Bi PCFLM is based on the interference between two counter-propagating beams in the fiber loop. The input light of the Hi-Bi PCFLM is spit into two counter-propagating beams with their individual polarization components by the 3-dB coupler, and they will propagate through the Hi-Bi PCF with different velocities. The above two beams will finally interfere when they recombine at the output port of the coupler. Therefore, the transmissivity of the Hi-Bi PCFLM could be given by [19]:

$$T(\lambda) = \frac{1 - \cos[\delta(\lambda)]}{2} \tag{1}$$

where $T(\lambda)$ is the transmissivity of a certain wavelength, and δ is the phase difference between the fast and slow beams propagating in the Hi-Bi PCF, which can be expressed as:

$$\delta(\lambda) = \frac{2\pi\Delta n L_B}{\lambda} \tag{2}$$

where Δn and L_B are the birefringence and the length of Hi-Bi PCF, respectively.

According to Eqs. (1) and (2), it is apparent that the transmission spectrum of the Hi-Bi PCFLM is periodic and the wavelength spacing between adjacent transmission peaks λ_T is determined by:

$$\lambda_T = \frac{\lambda^2}{\Delta n \, L_B} \tag{3}$$

Based on the above analysis, it is obvious that the transmissivity at a certain wavelngth is dependent on both of the birefringence and length of the Hi-Bi PCF. Hence, by correlating the birefringence or length of the Hi-Bi PCF with physical measurands via appropriate approaches, the Hi-Bi PCFLMs could be employed as fiber-optic sensors. This is the fundamental principle of Hi-Bi PCFLM-based sensors.

In order to achieve the measurement of displacement, 7.3 cm of the Hi-Bi PCF is pasted along the central axis of a UCB with a thickness of 4 mm and a length of 12.6 cm. For a UCB with L in length and h in thickness, the strain ε at any point along its central axis as a function of its free end displacement D can be described as [26]:

$$\varepsilon = \frac{hD}{L^2} \tag{4}$$

Therefore, by changing the free end displacement of the UCB, the fiber length along the central axis of the UCB will vary accordingly, leading to a transmission spectrum shift of the Hi-Bi PCFLM. Thus we could achieve displacement measurement by monitoring the wavelength shift via an optical spectrum analyzer (OSA) at the output port of the Hi-Bi PCFLM.

3. Experimental results and discussion

We have experimentally observed the spectrum evolution of the Hi-Bi PCFLM when the free end displacement of UCB increases from –21 mm (compression) to 21 mm (tension). Spectra *a*, *b*, *c* were measured at the displacements of –21 mm, 0 and 21 mm, respectively. By adjusting the polarization controller, the transmission loss of this sensor could be minimized to about 5 dB. The transmission spectrum is periodic with a peak wavelength spacing of ~35 nm. According to Eq. (3), it can be calculated that the PCF used in our experimental has a birefringence Δn of 6.13×10^{-4} at 1550 nm. Since strain is applied along the fiber axis, the change in birefringence could be neglected. In this case, the change in fiber length plays a major role in causing the shift of transmission spectrum. According to Eq. (2), when L increases, the transmission peak wavelength will also increase to maintain a constant phase. The above analysis is validated by the experiment results in Fig. 2. It can be seen that with the increase in displacement, both the transmission peak 1 and peak 2 move towards longer wavelength.
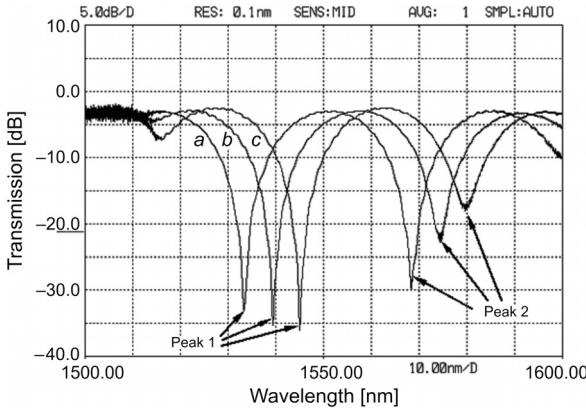
Fig. 2. Spectral response of Hi-Bi PCFLM at different displacements.
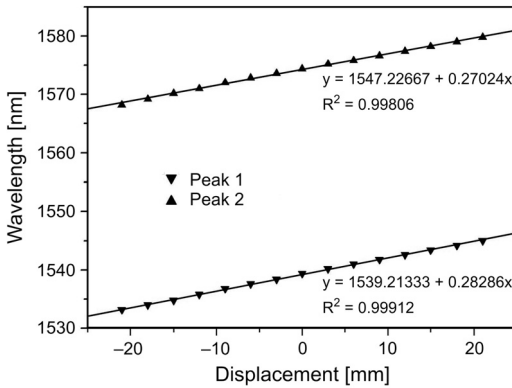

Fig. 3. Transmission peak wavelength of the Hi-Bi PCFLM as the function of displacement.

We have experimentally measured the wavelength shift of transmission peak 1 and peak 2 (as depicted in Fig. 2) at different displacements. Figure 3 shows the transmission peak wavelength as a function of displacement. It is apparent that both peak 1 and peak 2 linearly shift toward longer wavelength as the displacement increases. For peak 1 and peak 2, the sensing curves have good coefficients of determination of 0.99912 and 0.99806 with the sensitivity of 0.28286 nm/mm and 0.27024 nm/mm, respectively.

Based on Eqs. (1) and (2), transmission peak wavelengths with the lowest transmissivity satisfy the following equation:

$$\frac{2\pi \Delta n L_B}{\lambda} = 2k\pi \tag{5}$$

where k is a positive integer. Therefore, neglecting the change in birefringence and considering $L_B = L_1 + L_2$, where L_2 is the length of the fiber pasted on the UCB and L_1 represents the length of other Hi-Bi PCF that is not pasted, we have

$$\Delta n \frac{\Delta L_2}{L_2} = \frac{k\Delta\lambda}{L_2} \tag{6}$$

Based on Eqs. (4) and (6), the peak wavelength shift $\Delta\lambda$ as a function of displacement D could be expressed as:

$$\Delta\lambda = \frac{\Delta n\, L_2 h}{kL^2} D = k_D D \tag{7}$$

where $k_D = \Delta n L_2 h/kL^2$ is the proportional coefficient. Therefore, we have the final expression of peak wavelength:

$$\lambda = \lambda_0 + k_D D \tag{8}$$

where λ_0 is the initial peak wavelength. From the above analysis, it is clear that there is a linear relationship between the transmission peak wavelength shift and the free end displacement of UCB, which is in agreement with our experimental observation.

It should be noted that from Fig. 3, it is possible to obtain the dependence of fiber birefringence on displacement. According to Eq. (3), the fiber birefringence could be expressed as:

$$\Delta n = \frac{\lambda^2}{\lambda_T L_B} \tag{9}$$

Considering $L_B = L_1 + L_2$, for a strain of ε along the central axis of UCB, Eq. (9) could be modified as:

$$\Delta n = \frac{\lambda^2}{\lambda_T\left[L_1 + L_2(1 + \varepsilon)\right]} \tag{10}$$

According to Eq. (4), we have the birefringence of Hi-Bi PCF in terms of the free end displacement of UCB:

$$\Delta n = \frac{\lambda^2}{\lambda_T\left[L_1 + L_2\left(1 + \dfrac{hD}{L^2}\right)\right]} \tag{11}$$

Based on Eq. (11), we have calculated the fiber birefringence of the Hi-Bi PCF as a function of displacement of the UCB, as shown in Fig. 4. It can be seen that throughout the displacement range of –21 mm to 21 mm, the birefringence of the Hi-Bi PCF has a slight variation of no more than 1.377×10^{-5}. From Fig. 3, it can be seen that the two linear fitting curves are approximately in parallel and the fluctuation of λ_T throughout the displacement range is no more than 0.6 nm. Also, it should be noted that the variation of λ_T between adjacent displacement data points
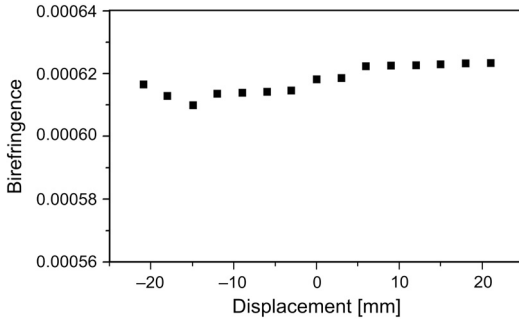
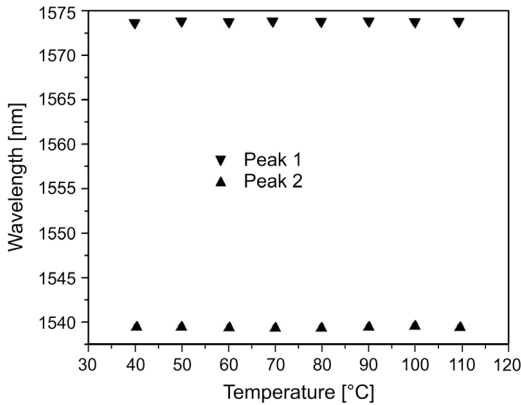Fig. 4. Calculated birefringence of the Hi-Bi PCF as the function of displacement.

Fig. 5. Temperature response of Hi-Bi PCFLM.

is no more than 0.2 nm, which is very close to the wavelength resolution of the OSA used in our experiment, and in this case the measured variation of λ_T would be affected by random noises and also in part depends on the measurement approach. Therefore, birefringence change of the Hi-Bi PCF is negligible for the measurement of displacement, as it has been treated in the above theoretical analysis.

Furthermore, by monitoring the wavelength shift of peak 1 and peak 2 without displacement at different temperatures, we also investigated the temperature stability of the Hi-Bi-PCFLM-based displacement sensor. Since the birefringence of Hi-Bi PCF is generally determined by its geometric asymmetry, the Hi-Bi PCF has a much more insensitivity to environmental temperature changes compared with conventional PMF-based FLMs. From Fig. 5, it can be seen that within a temperature range of 40 °C to 109.5 °C, the wavelength shifts of peak 1 and peak 2 are no more than 0.4 nm and 0.2 nm, respectively, which indicates that this displacement sensor is suitable for practical applications.

4. Conclusions

In summary, a fiber-optic displacement sensor based on Hi-Bi PCFLM is presented and experimentally demonstrated. By utilizing a UCB to change the length of Hi-Bi PCF, the relationship between the transmission peak wavelength of the Hi-Bi PCF and

the free end displacement of the UCB has been acquired. Experimental results indicate that this displacement sensor has fairly good coefficient of determination of 0.99912 and 0.99806 with the sensitivity of 0.28286 nm/mm and 0.27024 nm/mm over a displacement range of −21 mm to 21 mm for two adjacent peak wavelengths in the transmission spectrum, which is in agreement with our theoretical analysis. Peak wavelength measurement of the Hi-Bi PCFLM at different temperatures shows that it has also good temperature stability. The Hi-Bi-PCFLM-based displacement sensor with good linearity, temperature stability and low insertion loss is simple and cost effective, which ensures its feasibility for practical sensing applications.

References

[1] Zhang H., Yu L., Liu Y., Wang C., Li Y., Dou Q., Liu L., Yuan S., Dong X., *Noise figure improvement of a double-pass erbium-doped fiber amplifier by using a HiBi fiber loop mirror as ASE rejecter*, Optics Communications **244**(1−6), 2005, pp. 383−388.

[2] Li S., Chiang K.S., Gambling W.A., *Gain flattening of an erbium-doped fiber amplifier using a high-birefringence fiber loop mirror*, IEEE Photonics Technology Letters **13**(9), 2001, pp. 942−944.

[3] Liang D., Xu X., Li Y., Pei J., Jiang Y., Kang Z., Gao J., *Multiwavelength fiber laser based on a high-birefringence fiber loop mirror*, Laser Physics Letters **4**(1), 2007, pp. 57−60.

[4] Yan Y., Zhao Q., Chen S., Liu L., Zhang H., Dong X., *A novel variable optical attenuator and temperature sensor based on high-birefringence fiber-loop mirror*, Microwave and Optical Technology Letters **44**(3), 2005, pp. 259−261.

[5] Campbell M., Zheng G., Holmes-Smith A.S., Wallace P.A., *A frequency-modulated continuous wave birefringent fibre-optic strain sensor based on a Sagnac ring configuration*, Measurement Science and Technology **10**(3), 1999, pp. 218−224.

[6] Dong B., Zhao Q., Feng L., Guo T., Xue L., Li S., Gu H., *Liquid-level sensor with a high-birefringence-fiber loop mirror*, Applied Optics **45**(30), 2006, pp. 7767−7771.

[7] Marques B.V., Frazão O., Mendonça S., Perez J., Marques M.B., Santos S.F., Baptista J.M., *Optical current sensor based on metal coated Hi-Bi fiber loop mirror*, Microwave and Optical Technology Letters **50**(3), 2008, pp. 780−782.

[8] Zhang H., Liu B., Xiong L., Yu L., Dou Q., Chen S., Liu Y., Liu L., Yuan S., Dong X., *An all-fiber electric voltage sensor based on high birefringence fiber loop mirror*, Proceedings of SPIE **5623**, 2004, pp. 817−820.

[9] Frazão O., Silva S.O., Baptista J.M., Santos J.L., Statkiewicz-Barabach G., Urbanczyk W., Wojcik J., *Simultaneous measurement of multiparameters using a Sagnac interferometer with polarization maintaining side-hole fiber*, Applied Optics **47**(27), 2008, pp. 4841−4848.

[10] Sun G., Moon D.S., Chung Y., *Simultaneous temperature and strain measurement using two types of high-birefringence fibers in Sagnac loop mirror*, IEEE Photonics Technology Letters **19**(24), 2007, pp. 2027−2029.

[11] FRAZÃO O., MARQUES L.M., SANTOS S., BAPTISTA J.M., SANTOS J.L., *Simultaneous measurement for strain and temperature based on a long-period grating combined with a high-birefringence fiber loop mirror*, IEEE Photonics Technology Letters **18**(22), 2006, pp. 2407–2409.

[12] FRAZÃO O., EGYPTO D., ARAGÃO-BITTENCOURT L., GIRALDI M.T.M.R., MARQUES M.B., *Strain and temperature discrimination using high-birefringence erbium-doped fiber loop mirror with high pump power laser*, IEEE Photonics Technology Letters **20**(12), 2008, pp. 1033–1035.

[13] LIU Y., LIU B., FENG X., ZHANG W., ZHOU G., YUAN S., KAI G., DONG X., *High-birefringence fiber loop mirrors and their applications as sensors*, Applied Optics **44**(12), 2005, pp. 2382–2390.

[14] FANG X., CLAUS R.O., *Polarization-independent all-fiber wavelength-division multiplexer based on a Sagnac interferometer*, Optics Letters **20**(20), 1995, pp. 2146–2148.

[15] HAN Y., LI Q., LIU X., ZHOU B., *Architecture of high-order all-fiber birefringent filters by the use of the Sagnac interferometer*, IEEE Photonics Technology Letters **11**(1), 1999, pp. 90–92.

[16] MICHIE A., CANNING J., LYYTIKÄINEN K., ÅSLUND M, DIGWEED J., *Temperature independent highly birefringent photonic crystal fibre*, Optics Express **12**(21), 2004, pp. 5160–5165.

[17] ORTIGOSA-BLANCH A., DÍEZ A., DELGADO-PÍNAR M., CRUZ J.L., ANDRÉS M.V., *Temperature independence of birefringence and group velocity dispersion in photonic crystal fibres*, Electronics Letters **40**(21), 2004, pp. 1327–1329.

[18] STATKIEWICZ G., MARTYNKIEN T., URBAŃCZYK W., *Measurements of modal birefringence and polarimetric sensitivity of the birefringent holey fiber to hydrostatic pressure and strain*, Optics Communications **241**(4–6), 2004, pp. 339–348.

[19] ZHAO C., YANG X., LU C., JIN W., DEMOKAN M.S., *Temperature-insensitive interferometer using a highly birefringent photonic crystal fiber loop mirror*, IEEE Photonics Technology Letters **16**(11), 2004, pp. 2535–2537.

[20] KIM D.-H., KANG J.U., *Sagnac loop interferometer based on polarization maintaining photonic crystal fiber with reduced temperature sensitivity*, Optics Express **12**(19), 2004, pp. 4490–4495.

[21] FRAZÃO O., BAPTISTA J.M., SANTOS J.L., *Temperature-independent strain sensor based on a Hi-Bi photonic crystal fiber loop mirror*, IEEE Sensors Journal **7**(10), 2007, pp. 1453–1455.

[22] DONG X. TAM H.Y., SHUM P., *Temperature-insensitive strain sensor with polarization-maintaining photonic crystal fiber based Sagnac interferometer*, Applied Physics Letters **90**(15), 2007, p. 151113.

[23] HAN Y.G., *Temperature-insensitive strain measurement using a birefringent interferometer based on a polarization-maintaining photonic crystal fiber*, Applied Physics B **95**(2), 2009, pp. 383–387.

[24] FRAZÃO O., BAPTISTA J.M., SANTOS J.L., ROY P., *Curvature sensor using a highly birefringent photonic crystal fiber with two asymmetric hole regions in a Sagnac interferometer*, Applied Optics **47**(13), 2008, pp. 2520–2523.

[25] YANG X., ZHAO C., PENG Q., ZHOU X., LU C., *FBG sensor interrogation with high temperature insensitivity by using a HiBi-PCF Sagnac loop filter*, Optics Communications **250**(1–3), 2005, pp. 63–68.

[26] ZHANG W., WU Z., LIANG L., ZHAO Q., KAI G., LIU Z., DONG X., *Analyses and measurement of strain and deflection of standard beam based on fiber grating*, Proceedings of SPIE **4579**, 2001, pp. 269–273.